



Bioleaching to reprocess sulfidic polymetallic primary mining residues: Determination of metal leaching mechanisms



Agathe Hubau^{a,*}, Anne-Gwénaëlle Guezennec^a, Catherine Joulian^a, Carmen Falagán^b, David Dew^b, Karen A. Hudson-Edwards^b

^a Water, Environment and Ecotechnologies Division, BRGM, 3, Avenue Claude Guillemin, BP36009, Orléans 45060, Cedex 2, France

^b Environment & Sustainability Institute, Camborne School of Mines, University of Exeter, Penryn, Cornwall TR10 9FE, UK

ARTICLE INFO

Keywords:

Bioleaching
Nickel
Pyrrhotite
Chalcopyrite
Temperature
Mine waste

ABSTRACT

The mining of non-ferrous metals produces the largest volume of metal-containing, extractive waste in Europe, and about 29% of all the waste produced in the EU-28. In the framework of the European project NEMO (Near-zero-waste recycling of low-grade sulfidic mining waste for critical-metal, mineral and construction raw-material production in a circular economy), new ways to valorize sulfidic tailings are being developed through the recovery of valuable metals and critical raw materials and the transformation of the residual in clean mineral fraction to be used for the mass production of cement, concrete and construction products. The first step of the NEMO concept consists of removing the sulfides remaining from primary bioleaching and extracting the metals in the residual material (known as 'secondary ore') using either enhanced bioleaching or an alkaline autoclave conversion processes. This paper focuses on one of the project case studies, the secondary ore, obtained from an operating heap leaching plant (Terrafame, Finland). This material still contains several sulfide minerals (pyrrhotite, pyrite, sphalerite, pentlandite, violarite, chalcopyrite) and significant amounts of metals (Zn, Ni, Cu, Co, rare earth elements). The study aimed to characterize the mineralogy of the secondary ore and perform bioleaching in 2 L-stirred tank reactors, with three microbial cultures growing at 42, 48 and 55 °C. These results were compared to abiotic experiments, performed under the same conditions. Nickel was released very quickly, suggesting that part of Ni dissolved in the primary heap was re-precipitated and remained in the secondary ore. By contrast, Cu dissolution was much slower but the kinetics were substantially improved when the temperature was increased to 55 °C. Cobalt dissolution kinetics were highly improved by the bacterial activity, whatever the consortium. This is consistent with the presence of Co in the pyrite in the secondary ore.

1. Introduction

In Europe, most of the metal primary resources that have high or moderate metal grades and reasonable accessibility, and are easy to process, are exhausted. In today's context of resource scarcity, complex low grade ores and extractive wastes are receiving increasing attention. In particular, mining waste is being evaluated as a metal resource and as a material to be used in building and construction (Guezennec et al., 2015; Lèbre and Corder, 2015; Lottermoser, 2011; Matinde et al., 2018; Tayebi-Khorami et al., 2019). Different phenomena may emphasize the benefits of reprocessing mining wastes: (i) rising metal prices that increases the economic benefits from accessing lower cut-off grade thresholds; (ii) new and more efficient processing routes that did not exist when they were produced; (iii) extensive use of critical elements that were not of interest in the past. Many efforts are being made to

develop recycling or reuse options at reduced costs, with reduced environmental impacts and economic benefits. Large reprocessing operations have already been performed to reprocess gold mining wastes, as in Witwatersrand, South Africa or Mount Morgan, Australia for example (Bodéan et al., 2018). In Europe, reprocessing of mining waste operations are rare, with disseminated deposits and low economic value (Bodéan et al., 2018). Some operations have been or are active, as in Poland (for Zn recovery from Pb/Zn tailings by Zakłady Górniczo-Hutnicze), in Greece (for Au recovery in Olympias mine) and in Spain (for Sn and Ta in Penouta mine, from granitic ore, operated from 2011). Quantification of the elements in waste minerals and their distribution have been recognized as major challenges for the reprocessing of mining wastes (Lottermoser, 2011). Total elemental concentrations are often the only available information, with no or very few data on the occurrence of metals in mine wastes. In many cases, mine waste

* Corresponding author.

E-mail address: a.hubau@brgm.fr (A. Hubau).

<https://doi.org/10.1016/j.hydromet.2020.105484>

Received 15 May 2020; Received in revised form 2 September 2020; Accepted 15 September 2020

Available online 20 September 2020

0304-386X/ © 2020 The Authors. Published by Elsevier B.V. This is an open access article under the CC BY-NC-ND license (<http://creativecommons.org/licenses/by-nc-nd/4.0/>).

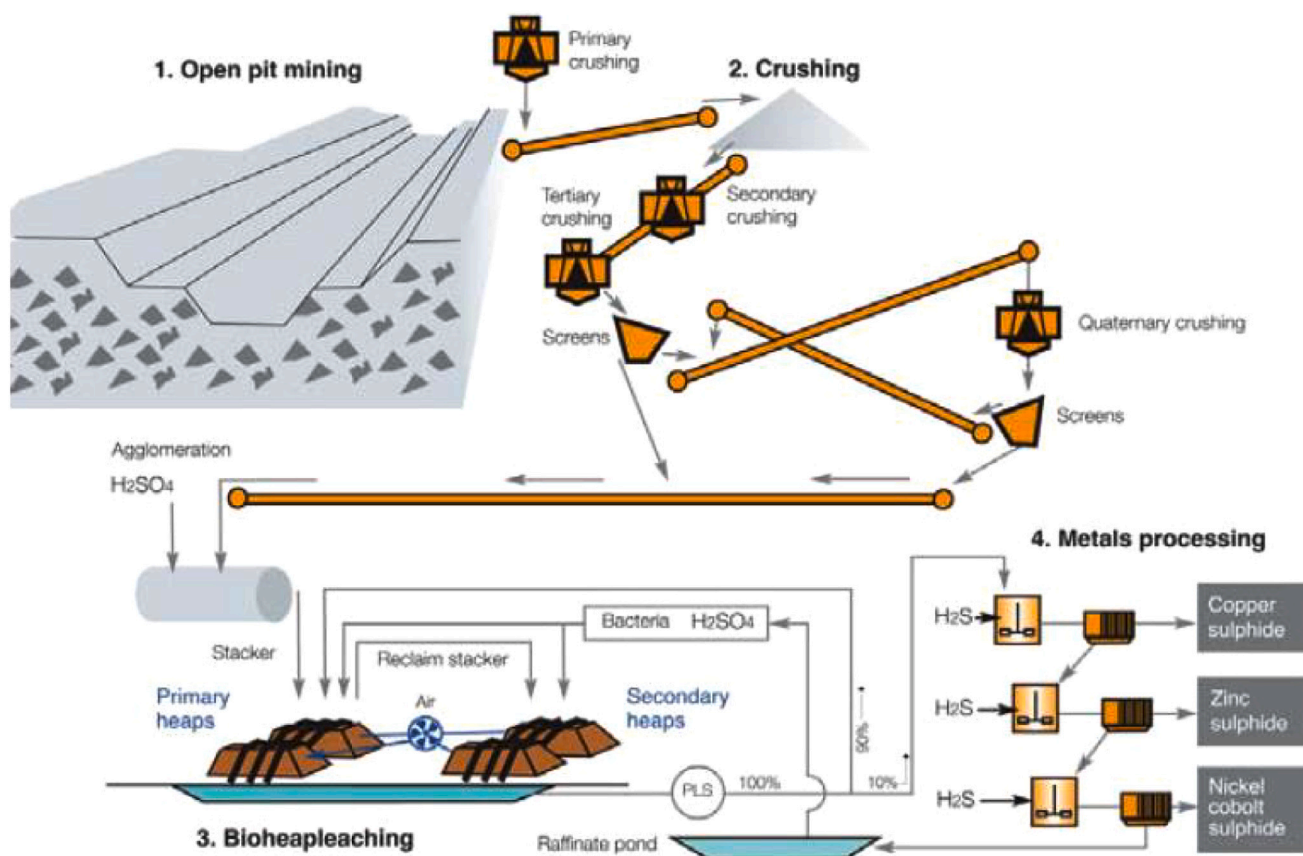


Fig. 1. Mining process in Sotkamo mine (Riekkola-Vanhanen, 2010).

mineralogy can be more complex than that of the primary ore, with the formation or disappearance of some species during the primary metal recovery process.

The European Commission supports many research projects to develop suitable technologies for reprocessing mine wastes, given that existing processes and technologies are often not profitable (Bodéan et al., 2018). Alternative routes need to be developed to address the complexity of composition while remaining cost effective. In this context, bio-hydrometallurgy is increasingly being recognized as an ecologically acceptable and yet economic alternative for the recovery of metals in low-grade sulfide materials. This technology was used at industrial scale to recover Co remaining in high sulfide flotation tailings from a former copper mine in Uganda (Morin and D'Hugues, 2007). The bioleaching plant produced 800 t/year of Co cathodes from 2001 to 2014 while preventing large environmental impact due to acid mine drainage by stabilizing the pyrite tailings. In Finland, an industrial bioleaching operation was performed by Mondo to valorize Ni from talc mining residues, and many other bioleaching reprocessing applications are being developed at laboratory scale (Neale et al., 2017; Falagán et al., 2017).

In addition to targeting metal extraction, sustainable development of biomining methods should also include an effective strategy to valorize the non-metallic fractions and thus to reduce drastically the generation of 'ultimate' wastes. The European research project NEMO (Near-zero-waste recycling of low-grade sulfidic mining waste for critical-metal, mineral and construction raw-material production in a circular economy) aims to valorize sulfidic mine wastes by combining innovative hydrometallurgical processes (including bioleaching) for the recovery of valuable metals and critical raw materials with the transformation of the residue in clean mineral to be used for mass production of cement, concrete and construction products (NEMO project, 2018).

This paper deals with the development of enhanced bioleaching

methods initiated in the framework of NEMO and aiming at recovering metals remaining in mine wastes. The wastes used in this study originated from Sotkamo mine (Terraframe, Finland) where bio-heap leaching is applied to process a pyrrhotite-rich pentlandite-containing black schist ore. At site, the bioleaching process is conducted in two steps (Fig. 1, Riekkola-Vanhanen, 2010): after crushing to less than 10 mm, freshly mined ore is continuously stacked on the Primary Leaching pad, which is operated as a dynamic pad, while the leach residue is continuously reclaimed (Arpalahti and Lundström, 2018). These residues, known as 'secondary ore', are only partially leached; they are stacked on the Secondary Leaching pad in multiple layers and submitted to secondary leaching to improve metal recovery. The residues (referred as 'secondary ore' in this paper) are presently around 5 Mt./year and remain permanently in the secondary heaps. The whole process is able to partially extract Ni, and Zn as well as Cu but to a lesser extent.

Numerous papers are devoted to the study of bioleaching of this ore in different configurations: in laboratory reactors (columns, air-lift, stirred tank), at pilot scale and during industrial full-scale operation (Ahonen and Tuovinen, 1995; Bhatti et al., 2010, 2012; d'Hugues et al., 2008; Dopson et al., 2008 Halinen et al., 2009a, 2009b, 2012; Niemelä et al., 1994. Puhakka and Tuovinen, 1986; Riekkola-Vanhanen, 2010). The most recent was published by Arpalahti and Lundström (2018) who studied the biogeochemical reactions that took place in primary heap leaching. They revealed that the presence of pyrrhotite makes it difficult to obtain high metals dissolution kinetics due to high acid consumption and the precipitation of metals within the primary heap. They were able to define clear strategies to maintain high efficiency of metal recovery whatever the heap age. These strategies are based on fine control of the aeration rate, acidification and irrigation rate.

Most of the literature devoted to this case study is focused on the primary ore, with very poor data on the bioleaching of the secondary

ore. As seen in the study of [Arpalahti and Lundström \(2018\)](#), one of the main challenges for reprocessing the secondary ore is the choice of the operating parameters. Temperature is one of the parameters that can have a strong impact on the bioleaching efficiency due to its influence on the composition and activity of microbial consortia, the kinetics of chemical reactions, the rate of formation of precipitates and the solubility of some elements (such as oxygen). Temperature also influences passivation occurring during the bioleaching of some sulfide minerals, such as chalcopyrite, which reduces the extent of their dissolution and the release of metals to solution. This phenomenon has been extensively reviewed ([Watling, 2006](#); [Kutschke et al., 2015](#)) and can be limited by fine control of the temperature ([Dew et al., 2000](#); [Gericke et al., 2001](#); [D'Hugues et al., 2002](#); [Hedrich et al., 2018](#)). Consequently, many studies have been carried out to determine the optimal temperature, either for an optimal growth and activity of the microbial species themselves, or for enhanced bioleaching performances from ores or concentrates ([Norris et al., 2017](#); [Watling et al., 2014](#)).

This paper investigates the dissolution and precipitation mechanisms involved in the bioleaching of a complex heap leach residue, known as 'secondary ore', and the influence of the temperature on the leaching efficiency by combining mineralogical characterization and classical bioleaching tests in batch stirred tank reactors (STR). The minerals present in the secondary ore were identified and quantified using quantitative evaluation of materials by scanning electron microscopy (QEMSCAN) and the occurrence of metals in the minerals was determined with scanning electron microscopy (SEM) and microprobe analysis. The growth and activity of three different consortia at different temperatures (42, 48 and 55 °C) were compared to assess their efficiency on the metal bioleaching kinetics and yields. Abiotic experiments were also included in the study in order to determine the contribution of chemical and biological mechanisms to metal bioleaching. The combination of these data shed light on the metal dissolution mechanisms that take place in the secondary ore during the bioleaching experiments.

2. Materials and methods

2.1. Geochemical and mineralogical analysis of secondary ore from Sotkamo mine

Experiments were performed using the secondary ore leach residue reclaimed from the primary bioleaching heap of Sotkamo mine (TerraFame, Finland). A sample of 30 kg of this secondary ore was provided by TerraFame, from which 15 kg were ground to a grain size of 500 µm with successive crushing and milling steps (Pinette and Henry jaw-crusher, roller mill and rod mill). The particle size of the ground secondary ore was determined by dry sieving and 80% of the particles had a size below 235 µm.

The chemical composition of Sotkamo secondary ore was determined in triplicate at BRGM using X-Ray Fluorescence (XRF; Zétium from Panalytical) for Al₂O₃, CaO, Fe₂O₃, K₂O, MgO, MnO, Na₂O, P₂O₅, and SiO₂, by potentiometry for Cl and NH₄⁺, by gravimetry for S⁰ and SO₄²⁻, by combustion for total S and by triacid leaching (HNO₃ – HClO₄ – HF) followed by inductive coupled plasma-optical emission spectrometry (ICP-OES, Horiba Jobin Yvon Ultima 2) and inductive coupled plasma mass spectrometry analysis (ICP-MS, Thermo Scientific X Series) for Co, Ni and Zn. Cu concentrations were determined with a 4 acid digestion followed by ICP-OES analysis (method ME-4ACD81 from ALS, Ireland). Sulfide concentrations were calculated by subtracting S⁰ and SO₄ concentrations from total sulfur.

The mineralogy of the Sotkamo secondary ore was determined using a QEMSCAN® 4300 at Camborne School of Mines (University of Exeter, UK) following the methodology outlined in [Rollinson et al. \(2011\)](#). The QEMSCAN® is equipped with a Zeiss Eco SEM and energy-dispersive X-ray (EDX) spectrometer. The X-ray data were collected every 10 µm across the sample surface. X-ray diffractometry (XRD; Siemens D5000

diffractometer) was performed as described in [Rollinson et al. \(2011\)](#). The XRD profiles were interpreted using the JCPDS PDF-2 2004 database and the method developed by [Bransgrove et al. \(2018\)](#) to differentiate the altered iron sulfides (FeS-alt) from other sulfides. The FeS-alt designates a mixture of elemental sulfur and sulfide and sulfate minerals (such as melanterite, coquimbite, schwertmannite and copiapite) resulting from the partial alteration of the TerraFame raw material sulfides during the primary bioleaching. The distribution of Ni, Cu, Co, Zn, Fe and Mn in selected minerals was determined using electron microprobe analysis (EMPA JEOL JXA-8200) and SEM-EDX analysis (Quanta FEG-SEM 650F). For the SEM-EDX, the beam was accelerated to 15 kV and focused at 13 mm. A 20 nA electron beam accelerated to 20 kV and focused to a 5 µm beam diameter were used for the EMPA and instrument was calibrated using a mixture of synthetic and natural minerals and pure metals.

2.2. Consortia and nutritive medium

The BRGM-KCC, TW48 and N55 consortia were compared to evaluate their ability to bioleach metals. The BRGM-KCC consortium, usually cultured at 42 °C ([Guezennec et al., 2017](#); [Guezennec et al., 2018](#)), originated from the BRGM cultures collection, was subcultured several times on cobaltiferous pyrite before being used as an inoculum for this study. It is mainly composed of the genera *Leptospirillum*, *Acidithiobacillus* and *Sulfobacillus*, which are either iron or sulfur-oxidizers, or both ([Guezennec et al., 2017](#)). The TW48 consortium was obtained in the frame of CeREs project (RFCS project contract n° 709868) by enrichment from a coal mining residue containing pyrite at 48 °C. The predominant microorganisms of this consortium were affiliated to the genera *Acidithiobacillus*, *Acidithiomicrobium* and *Sulfobacillus* ([Fonti et al., 2019](#)). The N55 consortium was derived from TW48 consortium, by subculturing TW48 at 55 °C on Sotkamo secondary ore.

The cultures were grown in a nutrient medium called '0Km' optimized for bacterial growth on sulfidic materials. Its standard composition is: (NH₄)₂SO₄, 3.70 g L⁻¹; H₃PO₄, 0.80 g L⁻¹; MgSO₄·7H₂O, 0.52 g L⁻¹; KOH, 0.48 g L⁻¹. Concentrated sulfuric acid (96% w/v) was used to adjust the pH of these media to 2.0.

The microbial inocula used in the bioleaching experiments were prepared by subculturing the consortia three times consecutively in 250 mL shake flasks on Sotkamo secondary ore (3% (w/v) solid) in an orbital shaking incubator at the following temperatures: 42 °C for BRGM-KCC, 48 °C for TW48 and 55 °C for N55.

2.3. Batch reactor experiments

2.3.1. Experimental setup

Bioleaching experiments were performed in batch mode in laboratory scale glass bioreactors with a working capacity of 2 L. These were jacketed for warm water circulation to maintain a constant operating temperature. The experimental setup is fully described in [Guezennec et al. \(2018\)](#). The temperature of the circulating water was controlled by a cryothermostat and thermocouples placed in the bioreactors. The bioreactors were equipped with four baffles mounted 90° apart and extended down to the base of the vessel to optimize the mixing of pulp. Agitation was performed using a dual impeller system (axial/radial) consisting of a standard 6-blade Rushton turbine combined with a 3-blade 45° axial flow impeller. The gas supply system was designed to accommodate air enriched with 1% CO₂ which was injected beneath the turbine at the bottom of the bioreactors via a stainless steel pipe. The impellers and the gas injection pipe were positioned in order to respect the standard dimensions and thus, to optimize gas mass transfer and mixing in the bioreactors. The top of the reactors was connected to a gas cooling system to prevent excessive evaporation.

2.3.2. Bioreactor monitoring

The cultures obtained in the shake flasks were used to inoculate a

first 2 L-STR. Then, for each batch test, the inoculum used was a sample of 200 mL of bioleached pulp taken at the end of the previous batch test. At the beginning of each test, the secondary ore was added to the nutritive medium and pH was adjusted to 2.0 with sulfuric acid. The inoculum was then added to the pulp. The pH was adjusted to 1.7. The stirring speed was maintained at 700 rpm. Daily monitoring was performed, including pH, redox potential, biomass concentration and metal concentrations measurements. Metal concentrations were measured with microwave plasma atomic emission spectroscopy (4210 MP-AES, Agilent Technologies). pH was manually adjusted to 1.7 with concentrated sulfuric acid when needed. Proton consumption was calculated from the initial pH of the nutritive medium. It resulted from the addition of the initial consumption when the solid was added, the pH monitoring over time and the acid addition. Water was also added to compensate water losses due to evaporation. All the tests lasted 2 weeks, unless otherwise specified. At the end of each experiment, the solid and the liquid phases of the bioleached pulp were separated by filtration on glass microfiber filters (from Ahlstrom, with pore size from 0.7 to 2.7 μm); the bioleached secondary ores were rinsed with acidified water (pH 1.7, sulfuric acid). For solid concentration above 5%, a solution containing 1 g.L^{-1} of flocculant (FA920) was added to the pulp to improve the filtration. The quantity was linearly adjusted to the solid concentrations to reach a ratio of 400 mg of flocculant per kg of materials. Bioleached secondary ores and filtrates were analysed to perform mass balances. The first tests were performed in triplicate. As the results were highly reproducible (Fig. S1), further tests were performed only once for logistical reasons.

2.3.3. Operating conditions

First, bioleaching experiments were carried out with BRGM-KCC, TW48 and N55 at 42, 48 and 55 $^{\circ}\text{C}$ respectively. The consortia were subcultured consecutively in 2 L-STR at 5% (w/w), 10% (w/w) and 10% (w/w) of the secondary ore in the OKm medium. The gas flow rate was maintained at 60 L.h^{-1} , with 1% CO_2 , and was chosen in order to avoid any oxygen or carbon limitations in the system.

Three experiments with no added inoculum (hereafter referred to as abiotic experiments) were also performed at 10% (w/w) solid, at 55 $^{\circ}\text{C}$. In the first test, the operating conditions were the same as those of the biotic tests without any inoculum. In the second test, the solid was sterilised with autoclaving 3 times at 110 $^{\circ}\text{C}$ during 30 min to limit the number of viable bacteria carried by the material and to avoid contamination. In the third test, the nutritive medium was replaced by acidified water (pH 1.7) to limit contamination and to ensure that the mineralogy of the secondary ore was not modified by autoclaving. Before conducting these experiments, reactors and gas pipes were sterilised by autoclaving. Fresh nutritive medium and injected gas were filtered at 0.2 μm . After the addition of solid to the medium, 200 mL of a 1 g.L^{-1} Fe(III) solution at pH 1.7, prepared from $\text{Fe}_2(\text{SO}_4)_3 \cdot x\text{H}_2\text{O}$ and from concentrated sulfuric acid and filtered at 0.2 μm , was added in each STR, which corresponds to the amount of Fe(III) brought by the inoculum in the biotic tests. The biotic reactor used for the comparison was performed with the N55 consortium at 10% (w/w). In these experiments, the gas flow rate was 120 L.h^{-1} enriched with 1% CO_2 to avoid plug-in phenomena encountered in the first set of bioleaching tests.

2.4. Bacterial community monitoring

The number of micro-organisms in the supernatant was monitored by microscopic counting on Thoma cell counting chamber. For DNA-based gene quantification and fingerprinting methods, 2 mL of pulp was taken from the 2 L-reactors and was centrifuged for 10 min at 14,000 g. Pellets were washed by re-suspension in 1 mL tris(hydroxymethyl) aminomethane buffer (100 mM, pH 8) until the pH reached around 7 and stored at -20°C prior to DNA extraction. Microbial DNA was extracted from the washed pellets with the FastDNA Spin Kit for Soil

and using the manufacturer's protocol (MP Biomedicals) with a FastPrep[®]-24 instrument at a speed of 5 m.s^{-1} for 30 s. To complement microscopic cell counts, quantitative *real-time* polymerase chain reaction (qPCR) assays targeting the bacterial 16S rRNA gene were used to estimate bacterial biomass, using primers 341F and 534R and the procedure described by Hedrich et al. (2016). Real-time data and gene copies numbers were obtained with the CFX Manager software (BioRad), and the results were expressed as gene copies per mL of pulp. The CE-SSCP fingerprinting technique was applied on the V3 region of 16S rRNA genes, amplified by PCR with w49 forward primer and 5'-end FAM-labeled w34 primer, to obtain a diversity profile and to determine relative abundances of the detected bacterial strains, as in Hedrich et al. (2016). The software Bionumerics (Applied Maths) was used to realign the peak profiles and assign peak position based on internal standard migration, calculate relative abundances on the basis of peak heights, and compare with peak profile of reference bioleaching strains.

3. Results

3.1. Geochemistry and mineralogy of the Sotkamo secondary ore

The geochemical results for the Sotkamo secondary ore used in this study are shown in Table 1. The material contained high content of sulfate (40% of total S) and sulfide (45% of total S), and smaller quantities of elemental sulfur (15% of total S).

The mineralogical analysis of the secondary ore is presented in Table 2. The minerals identified by XRD were quartz, microcline, clinocllore Iib-2, gypsum, tremolite, anhydrite, pyrite, jarosite, albite, clinocllore, biotite and phlogopite. Mineral quantification with QEMSCAN[®] identified quartz, K-feldspar, FeS-alt, jarosite, plagioclase, phlogopite and tremolite as the main minerals (Table 2). The combined mass of sulfide minerals accounted for 15.2% of the total, with FeS-alt (12.0%) and pyrite (2.5%) being the most dominant phases. Fig. 2 shows the distribution of the different sulfides within the secondary ore. EMPA analysis suggested that the FeS-alt correspond to iron oxyhydroxysulfates mainly (Table S1), and that the Fe-Ox/ CO_3 phases were attributed to Fe oxides, hydroxides or oxyhydroxides such as goethite.

Copper occurred in discrete particles of chalcopyrite (33.8 wt%), in pyrrhotite (0.04 wt%), in the FeS-alt (up to 0.19 wt%) and in one grain of the Fe-Ox/ CO_3 (0.03 wt%). Violarite contained the highest concentration of Co (3.6 wt%) but only one grain of this mineral was found. Pyrite, pyrrhotite, the FeS-alt and the Fe-Ox/ CO_3 contained minor amounts of Co (0.09–1.27 wt%, 0.07–0.13 wt%, up to 0.08 wt% and up to 0.08 wt%, respectively, Table S1). Violarite and pentlandite were the main Ni-bearing minerals, and Ni was also detected in the FeS-alt (up to 0.33 wt%) and in one grain of the FeOx/ CO_3 phases (0.06 wt%). The major Zn-bearing mineral was sphalerite, which also contained high concentrations of Mn (4.3–6.8 wt%) and Fe (7.1–9.8 wt%). Zinc was also found in the FeS-alt (up to 0.40 wt%) and in the FeOx/ CO_3 (up to 0.61 wt%) (Table S1).

Table 1

Total elemental concentrations of the secondary ore from Sotkamo mine.

Element	Concentration (mg.kg^{-1})	Element	Concentration (mg.kg^{-1})
Al	50,000 \pm 0.3%	Na	2940 \pm 4.8%
Org C	67,800 \pm 0.2%	NH_4	1.51 \pm 2.3%
Ca	21,100 \pm 0.5%	Ni	1310 \pm 11%
Cl	3700 \pm 33%	P	1280 \pm 0.7%
Co	175 \pm 10%	S as SO_4	21,500 \pm 13%
Cu	1370 \pm 1.5%	S as S^0	8330 \pm 13%
Fe	75,300 \pm 0.5%	S as $\text{S}^=$	26,100 \pm 14%
K	26,200 \pm 0.2%	Total S	57,000 \pm 2.2%
Mg	18,900 \pm 0.3%	Si	215,000 \pm 0.3%
Mn	3180 \pm 0.0%	Zn	3460 \pm 13%

Table 2
QEMSCAN® mineral apportionment in the secondary ore from Sotkamo mine.

Mineral	Wt%	Mineral	Wt%
Pyrite	2.45%	Gypsum	2.70%
Pyrrhotite	0.30%	Fe-Ox/CO3	2.69%
Altered Fe sulfides	11.97%	Biotite	0.97%
Jarosite	11.21%	Chlorite	2.72%
Sphalerite	0.20%	Tremolite	4.03%
Chalcopyrite	0.17%	Quartz	24.72%
Pentlandite	0.01%	K-feldspar	14.79%
Violarite	0.06%	Plagioclase	8.27%

3.2. Selection of microbial consortia for efficient bioleaching of Sotkamo material

The influence of the temperature and, consequently, of the consortium composition, on the bioleaching efficiency were assessed. Three successive subcultures of each consortium were performed at increasing solid concentrations to favor the adaptation of the microorganisms (Hedrich et al., 2016). The results that are presented in this section were obtained on the third subculture, which showed the best adaptation to the Sotkamo secondary ore. For this subculture, the biomass concentration in the three inocula reached between $1.5 \cdot 10^9$ and $1.9 \cdot 10^9$ cell.mL⁻¹ in the liquid phase.

The increase of the redox potential, which denotes the microbial activity of Fe-oxidizing microorganisms (Nemati and Webb, 1997), was faster in the bioreactors inoculated with BRGM-KCC compared to those inoculated with TW48 and N55 (Fig. 3). The proton consumption was lower at 42 °C than at 48 and 55 °C. All of the experiments showed similar degrees of microbial growth (Fig. S2).

As shown in Fig. 4A and Fig. 4B, Ni, Zn and Co dissolution kinetics were similar and were independent on the type of consortium and the temperature. Metals were noticeably released in solution at the

beginning of the experiments, before inoculation. Nickel, zinc and cobalt dissolution yields reached approximately 48%, 15% and 20%, respectively, when the solid was suspended in nutritive medium (in less than 30 min; Fig. 5). After inoculation, Zn and Ni dissolution kinetics remained fast (approximately 3.7 and 1.4 mg.L⁻¹.h⁻¹ respectively), while Co dissolution stopped before increasing again from day 3 with a linear trend over time. The final yield was close to 90% for Ni, 85% for Zn, and 75% for Co after 14 days (Fig. 5). Cu leaching kinetics were much slower compared to the Ni and Zn leaching kinetics, but, in contrast to the other metals, increasing the temperature had a positive impact on the leaching yield, which reached 50% for N55 at 55 °C after 14 days. The yield reached only 40% for BRGM-KCC at 42 °C and 47% for TW48 at 48 °C.

As seen in Fig. 5, elemental sulfur and sulfide oxidation yields were not influenced by the temperature and reached respectively 45% and 80%. The speciation of the bioleached secondary ores was 64% of S as SO₄²⁻, 16% as S⁰ and 20% as S²⁻.

Iron concentrations increased during the first day and followed similar dissolution kinetics in the three experiments (Fig. 4C). After the dissolved Fe concentration reached 2000 mg.L⁻¹, corresponding to an Fe yield of approximately 20%, it then remained constant until the end of the experiment with BRGM-KCC consortium at 42 °C. In the case of the TW48 and N55 consortia, Fe concentrations decreased from day 3 to the end. This phenomenon was probably linked to the precipitation of Fe(III) as jarosite or another Fe(III) phase such as goethite. This decrease was more pronounced at 55 °C.

Sulfate concentrations in the liquid phase were monitored during the experiment with the N55 consortium (Fig. 6). These concentrations were compared to sulfate concentrations from the 0Km medium and from the sulfuric acid used to control the pH. Sulfate concentration rapidly increased in the culture medium when the solid was suspended in the bioreactor, prior to inoculation. This was probably due to sulfate dissolution from the secondary ore, rather than sulfur or sulfide

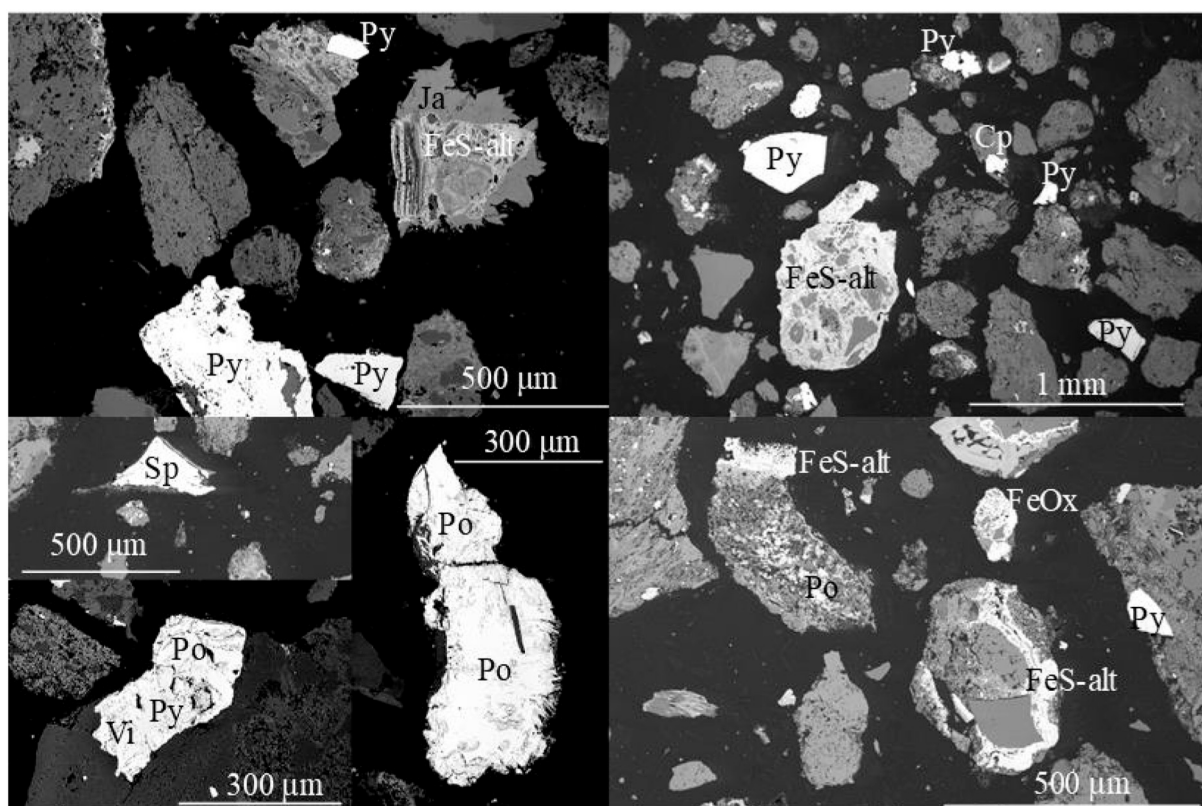


Fig. 2. SEM image identifying sulfide mineral phases and iron oxides in secondary ore particles. Pyrite (Py), pyrrhotite (Po), violarite (Vi), chalcopyrite (Cp), sphalerite (Sp), jarosite (Ja), iron oxides (FeOx) and altered iron sulfides (FeS-alt).

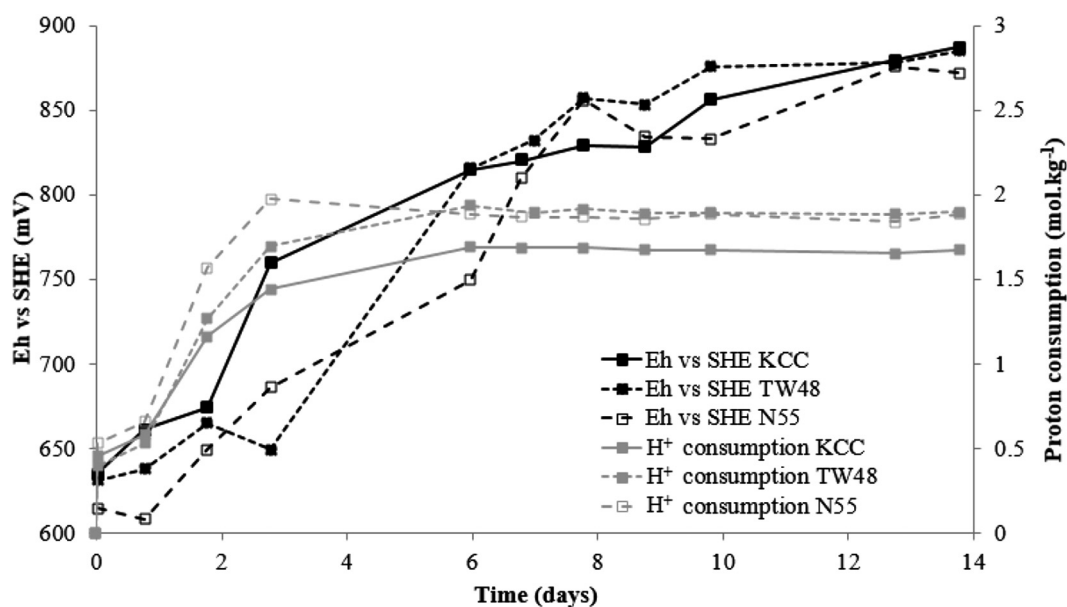


Fig. 3. Redox potential and protons consumption over time for the experiments with the three different consortia at 42, 48 and 55 °C.

microbial oxidation since the reactor was not inoculated. After 24 h, the sulfate concentration measured in the solution became slightly lower than the sulfate concentration calculated as the sum of sulfate coming from the nutrient solution, the added H₂SO₄ and the sulfate released at the beginning of the experiment. This suggests that some sulfates disappeared from the liquid phase (10 mmol.L⁻¹), possibly due to the precipitation of jarosite [KFe₃(SO₄)₂(OH)₆], which is a common phase that precipitates in acidic (pH 2–4), Fe- and sulfate-rich solutions (Dutrizac and Jambor, 2000). According to jarosite chemical formula, 3 mol of Fe with 2 mol of sulfate are required to form 1 mol of jarosite. Based on the disappearance of sulfate from the liquid phase, we can assume that 5 mmol.L⁻¹ of jarosite was formed from day 2 to day 4, which corresponds to a theoretical consumption of 15 mmol.L⁻¹ of Fe. In the meantime, 13.5 mmol.L⁻¹ of Fe were removed from the liquid phase. This quantity was slightly lower than the stoichiometric quantity for jarosite formation, but this may be explained by the simultaneous dissolution of Fe from other minerals, such as pyrite, or by the fact that jarosite normally forms with Fe vacancies in its structure, giving ratios of Fe:SO₄ lower than 3:2 (Kubisz, 1970).

Fig. 7 shows that the consumption of K and P from the liquid phase raised with temperature. It may be due either to an increase of nutrients consumption by the consortia, or to precipitation (e.g., of K in jarosite) or sorption phenomena (e.g., of phosphate sorbed on goethite in the secondary ore) promoted by higher temperature (Dutrizac and Jambor, 2000; Ioannou et al., 2013).

Increases in temperature resulted in a slight increase of the dissolution yields of Al, Mg and Mn which might be related to the leaching of the gangue minerals present in the secondary ore. Halinen et al. (2009b) performed column bioleaching experiments with Sotkamo primary ore and already denoted higher dissolution of these cations at 50 °C than at lower temperature. The decrease of Ca dissolution yield at 55 °C may result from partial precipitation of dissolved Ca.

Diversity fingerprints of the third subculture in 2 L reactors showed clear differences between BRGM-KCC on the one hand and TW48 and N55 on the other hand (Fig. 8). BRGM-KCC cultured at 42 °C comprised the three bacteria usually found in this consortium: the autotrophic iron-oxidizer *Leptospirillum* (*L.*) *ferriphilum* BRGM1, the iron- and sulfur-oxidizer *Sulfobacillus* (*Sb.*) *thermosulfidooxidans* and the sulfur-oxidizer *Acidithiobacillus* (*At.*) *caldus* (Guezennec et al., 2017). One singularity is the detection of two different sequences of *Sb. thermosulfidooxidans*, B1 and B33 that may correspond to two strains of this species. A fifth strain

(UN1 on Fig. 8) is found, most probably another strain of *At. caldus*, as it is analogous with previous fingerprints of the BRGM-KCC consortium that showed two signals corresponding to *At. caldus* (D'Hugues et al., 2007). This cannot be fully confirmed here because a reference strain is lacking. In terms of relative abundance, *L. ferriphilum* formed only a minor proportion of the consortium and at times was undetectable during the monitoring. The bioleaching community was dominated by strains of *Sb. thermosulfidooxidans* and the fifth strain UN1.

Four strains were detected in the TW48 consortium cultured at 48 °C: *Sb. thermosulfidooxidans* B1, a moderate thermophilic and autotrophic iron- and sulfur-oxidizer '*Acidithiobacillum*' P2 (Norris et al., 2011), *L. ferriphilum* and the UN1 strain also found in BRGM-KCC. At Day 0, *Sb. thermosulfidooxidans* B1 was dominant over strain UN1, '*Acidithiobacillum*' P2 and traces of *L. ferriphilum*. *Sb. thermosulfidooxidans* B1 and strain UN1 remained main actors, but the proportion of '*Acidithiobacillum*' P2 increased from Day 8 to be the dominant strain (60%) at the end of the bioleaching experiment. A small proportion of an unidentified bacterium was also detected on Day 1.8. This bacterium may have been indigenous to the Sotkamo ore if the strain was present in situ.

Only two bacteria were detected in the N55 consortium at 55 °C: '*Acidithiobacillum*' P2 and *Sb. thermosulfidooxidans* B1. The consortium was dominated by '*Acidithiobacillum*' P2 at the start of the experiment (70% at day 0), and then by *Sb. thermosulfidooxidans* B1 (> 90% at day 1.8 and 7.8). At the end of the experiment, the proportions were more equal, at 47% ('*Acidithiobacillum*' P2) and 53% (*Sb. thermosulfidooxidans* B1). This diversity was similar to the structure of the TW48 consortium from which it was derived.

3.3. Comparison of leaching efficiency in biotic and abiotic experiments

Abiotic experiments were used to compare metal dissolution kinetics in the presence and absence of added microorganisms. Three abiotic experiments were performed at 55 °C, since this temperature favored Cu dissolution: (i) one with 0Km and original solid, i.e. the same operating conditions were implemented but any inoculum was added; (ii) one with 0Km and sterilised solid, to limit the number of viable bacteria carried by the Sotkamo material; and (iii) one with acidified water and the original solid. Sterilization of the secondary ore was performed by autoclaving. This technique might change mineralogy of the ore. The conditions of the third type of abiotic tests were

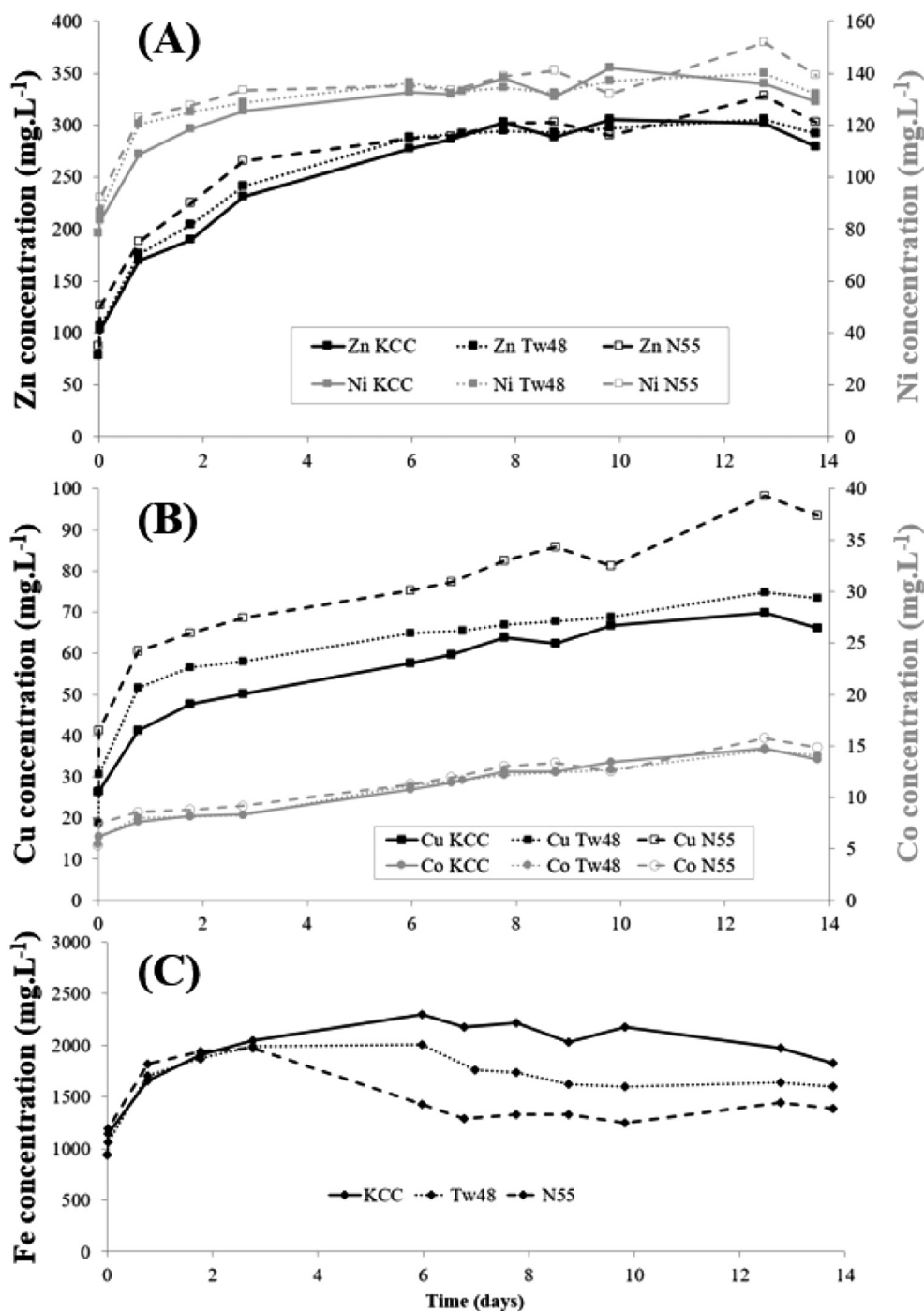


Fig. 4. Zn, Ni (A); Cu, Co (B) and Fe(C) concentrations versus time for the bioleaching experiments with the three consortia.

selected to avoid any modifications of the mineralogy while preventing the development of microorganisms potentially present on the original materials thanks to the absence of nutrients. The results were compared to the biotic experiment performed with the N55 consortium under the same operating conditions (55 °C and 10% (w/w) solid).

As seen in Fig. 9, redox potential exhibited a sharp increase after 8 days in the abiotic experiment performed with OKm medium and original materials, and after 11 days for the abiotic experiment performed with OKm medium and autoclaved materials. The rise in Eh was similar in the biotic and the two abiotic tests carried out with nutrients, even though the rise was delayed in the abiotic tests. This trend is typical of a microbial iron-oxidizing activity with a first period of low redox potential corresponding to the microbial lag phase followed by a

quick increase of the redox potential corresponding to the exponential phase when the bacteria are growing exponentially and thus are oxidizing ferrous iron very quickly. In contrast, the Eh increased slowly and almost linearly in the abiotic experiment performed with the original secondary ore and no nutrients. In this case, the rise in Eh can be attributed to the chemical oxidation of Fe by oxygen, whose kinetics are very slow compared to those of the biological oxidation of Fe (Lacey and Lawson, 1970). The changes in Eh over time suggest that biomass development occurred in the abiotic tests performed with OKm medium (original materials and autoclaved materials), whereas this development was almost inexistent or remained very low in the abiotic test performed without nutrients.

The Eh trend also correlated with proton consumption (Fig. 9);

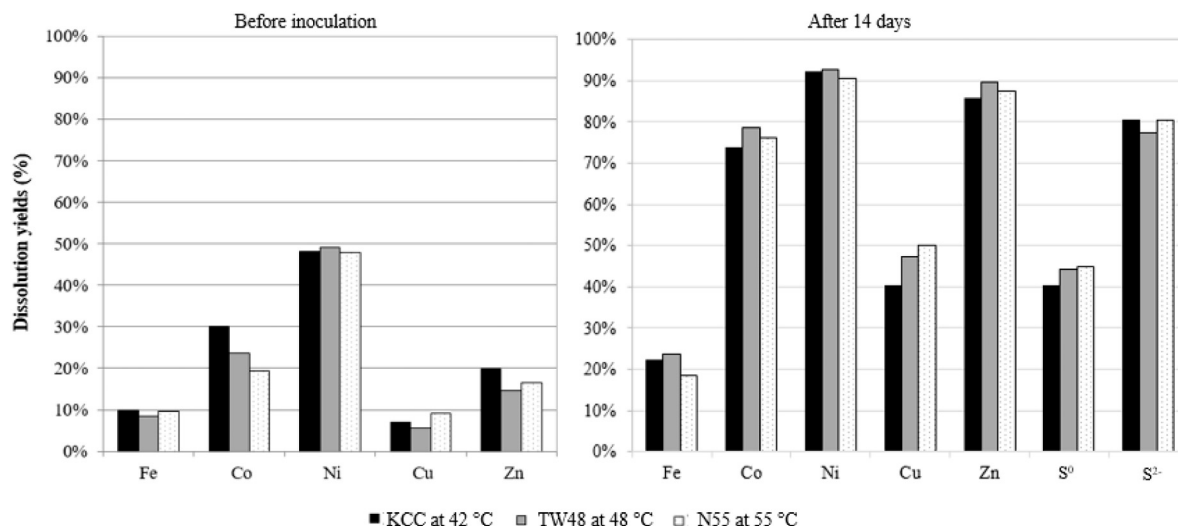


Fig. 5. Dissolution yields before inoculation (calculated from the analysis of the leaching solution, left) and after 14 days (calculated from the analysis of the leaching residues, right) for the three consortia.

when the Eh started to increase in the abiotic tests performed with nutrients, proton consumption stopped. A similar phenomenon occurred in biotic tests and denoted the development of sulfur-oxidizing microorganisms which produce sulfuric acid and contribute to maintaining the pH at 1.7. In the abiotic test performed without nutrients, the proton consumption increased during the whole duration of the test.

The development of the biomass was confirmed by the monitoring of gene abundance as a biomass estimate. The presence of bacteria was detected in all abiotic reactors after 14 days of the experiment. In the test performed with the original material but without nutrients, the biomass concentration was about two orders of magnitude lower than in biotic test (2.3×10^5 and 3.4×10^7 gene copies.mL⁻¹ pulp at Day 14, respectively) and remained quite stable until the end of the experiment (5.7×10^5 copies.mL⁻¹ pulp at 24 days). In contrast, a significant growth of the biomass was measured in the abiotic tests performed with nutrients (original materials and autoclaved materials), and gene abundance reached the same level in both types of experiments (2.0×10^7 and 3.0×10^7 copies.mL⁻¹ pulp at 14 days, stable until the end). In terms of diversity, the iron- and sulfur-oxidizing strain *Sb. thermosulfidooxidans* B1 was the only strain detected in the abiotic tests. As the reactors were not inoculated, this bacterium could have been indigenous to the Sotkamo secondary ore. However, the

possibility of contamination of the vessels cannot be excluded, since *Sulfobacillus* are spore formers and may thus have survived to sterilization by autoclaving of the reactors and gas pipes (Johnson et al., 2008; Watling et al., 2008). These results confirmed the presence of bioleaching bacteria and their better development when nutrients were available. It also suggest that Sotkamo secondary ore sterilization by autoclaving may not have been sufficient to avoid the development of endogenous bacteria when 0Km medium was used.

Copper dissolution kinetics and final yield (Fig. 10A and Fig. 11) were similar in the abiotic and biotic experiments, suggesting that the microorganisms were not involved in the leaching of the Cu-bearing phases. The rapid release of Ni and Zn at the beginning of the tests was similar in the abiotic and biotic experiments (Figs. 10B). After a few days, Ni and Zn dissolution slowed down in the abiotic tests compared to the biotic test and the final Ni and Zn yields were lower than in the biotic test. A similar trend was observed for Co, but with a more pronounced difference in the dissolution kinetics and final yield between the two experiments (Fig. 10C and Fig. 11). During the first four days, Co release was the same in the biotic and abiotic tests. Subsequently, Co dissolution ceased in the abiotic tests whereas it sharply increased in the biotic tests. After 9 days, Co dissolution increased again in the abiotic tests performed with the original material in 0 Km medium. A

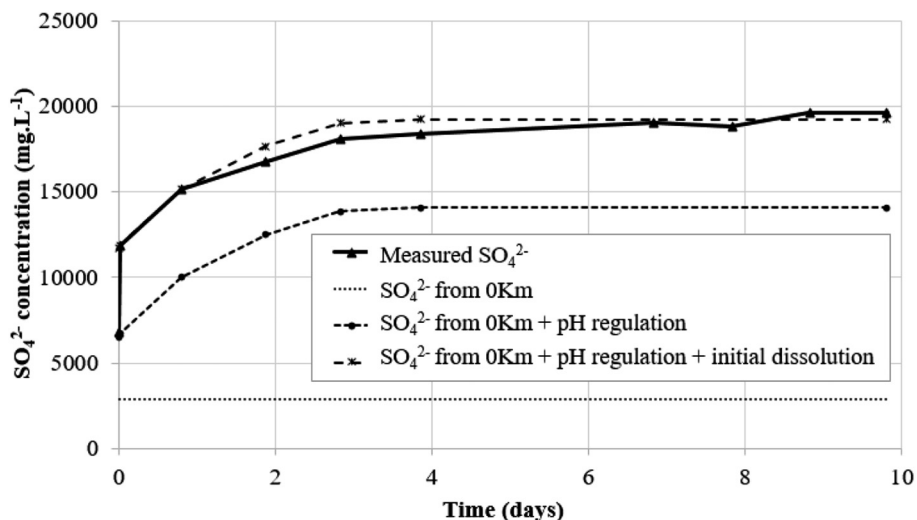


Fig. 6. Sulfate concentrations in the liquid phase versus time in a bioreactor with N55 consortium at 55 °C and 10% solid.

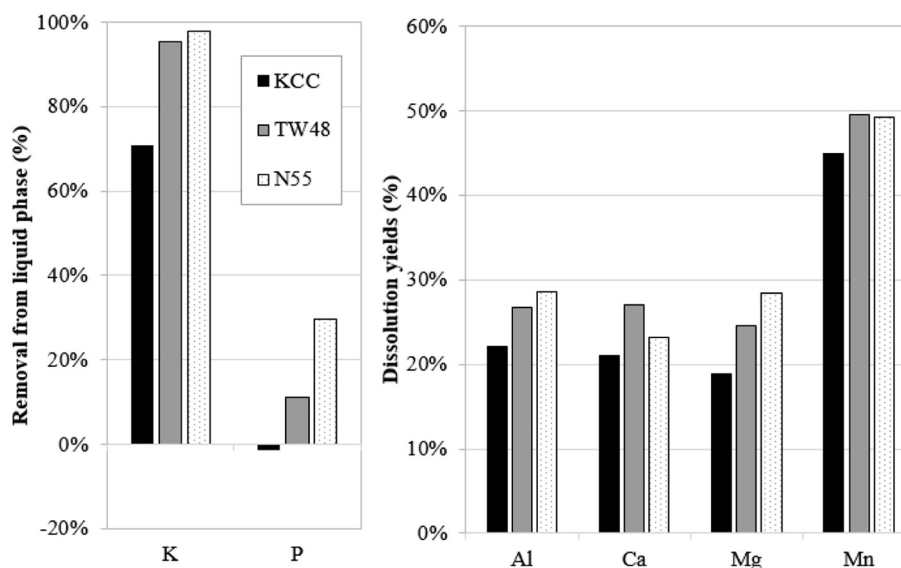


Fig. 7. K⁺ and P (from PO₄³⁻) removed from the liquid phase (left) and dissolution yields for gangue elements after 14 days (right) for the three consortia.

similar increase was observed in the test carried out with the autoclaved material in OKm medium, but only after 11 days. In the test performed with the original material in acidified water, Co dissolution increased, but at a much slower rate compared to the other tests. Cobalt dissolution kinetics were well correlated with the Eh changes over time in the abiotic and biotic tests, increasing as Eh increased (Fig. 9).

Sharp decreases in the Fe concentration were correlated with Eh increases, especially in the biotic test and in the abiotic tests performed with nutrients (original materials and autoclaved materials) (Fig. 10D). These decreases are likely due to the oxidation of Fe, which subsequently precipitated as jarosite or another Fe(III)-bearing phase. The abiotic experiment conducted without nutrients did not show a sharp increase in Eh.

Sulfide was dissolved in high proportions in all abiotic experiments, but the development of the biomass in those performed with nutrients slightly increased the final dissolution yields (81% in the test without nutrients, and 94% in the tests with nutrients, Fig. 11). In contrast to sulfide, the amount of elemental sulfur dissolution was significantly different between the abiotic test without nutrients and with nutrients. In the former, the final sulfur yield was negative after 24 days, suggesting the production and precipitation of elemental sulfur. Fifty % of the elemental sulfur was dissolved in OKm medium abiotic tests. These results confirm that the development of the biomass in the abiotic tests without nutrients was too low to enable the oxidation of the sulfur and the production of sulfuric acid.

4. Discussion

Bioleaching experiments in 2 L batch reactor with Sotkamo secondary ore were characterized by some common features regardless of the operating conditions implemented.

First, all experiments exhibited a first period of time of 3 to 4 days characterized by low Eh conditions (between 550 and 650 mV SHE) and high acid consumption. During this period, the pH increased between daily acid additions. After this first period, the Eh increased sharply whereas the pH decreased and acid addition was not necessary any longer. The Eh and pH then stabilized around 850 mV and 1.6 respectively. The microbial growth trend was similar with some slight differences. In particular, the first period was generally shorter, a substantial increase in biomass being observed after 2 days. Usually, in most bioleaching batch tests in STR, the lag phase of the microbial growth phase corresponds to the period of low Eh and the exponential growth phase corresponds with a sharp Eh increase. In the current tests

with the Sotkamo secondary ore, the increase of Eh was delayed following the end of the lag phase of the microbial growth. This trend is typical of the presence of minerals such as pyrrhotite or other acid soluble sulfides, such as the FeS-alt detected by QEMSCAN in Sotkamo secondary ore. Two hypothesis can be raised to explain this difference:

- (i) Between the beginning of the exponential microbial growth phase and the increase in solution redox potential, the microbial oxidizing activity for Fe(II) oxidation was low to counterbalance chemical leaching mechanisms: that is, the rate of Fe and S biooxidation was lower than the consumption of Fe(III) and sulfuric acid by the chemical dissolution of minerals. This effect would explain the initial low Eh (i.e. most of iron was present as Fe(II)) and that continued acid addition was required, in order to maintain the pH at the appropriate level (below 1.8).
- (ii) Dissolution of pyrrhotite releases H₂S even under aerobic conditions, which could have contributed to the reduction of iron and therefore delayed the redox increase after the end of the lag phase.

It is likely that during the first two days corresponding to the lag phase, the microbial activity was very low or almost non-existent and the leaching mechanism was purely chemical. Then, at the beginning of the exponential growth phase, the redox remained low because of the mechanisms described above. When Eh increased, it can be assumed that most of pyrrhotite was leached, and acid insoluble minerals such as pyrite started to dissolve due to the presence of Fe(III) (Arpalahti and Lundström, 2018; Miller et al., 1997). During pyrite leaching, Fe(III) consumption was slower than Fe oxidation catalysed by microorganisms which allowed high Eh to be maintained.

Another important feature was the substantial and rapid release of metals at the very beginning of all leaching experiments and confirmed by separate ore washing tests. Around 55% of Ni, 25% of Co, 20% of Zn and 10% of Cu were dissolved almost instantaneously when the secondary ore was added to the medium prior to inoculum addition. Simultaneous to metal dissolution, sulfate also dissolved in the liquid phase. This phenomenon suggests that a portion of the metals contained in Sotkamo secondary ore is in the form of soluble salts, which is consistent with the observations of Arpalahti and Lundström (2018). These authors studied the leaching mechanisms encountered in operation of the Sotkamo primary heap and noticed that metals dissolved from sulfide minerals may precipitate within the heap, particularly in dry areas where the irrigation is poor. These metals remain in the reclaimed material as secondary ore that feed the secondary heap.

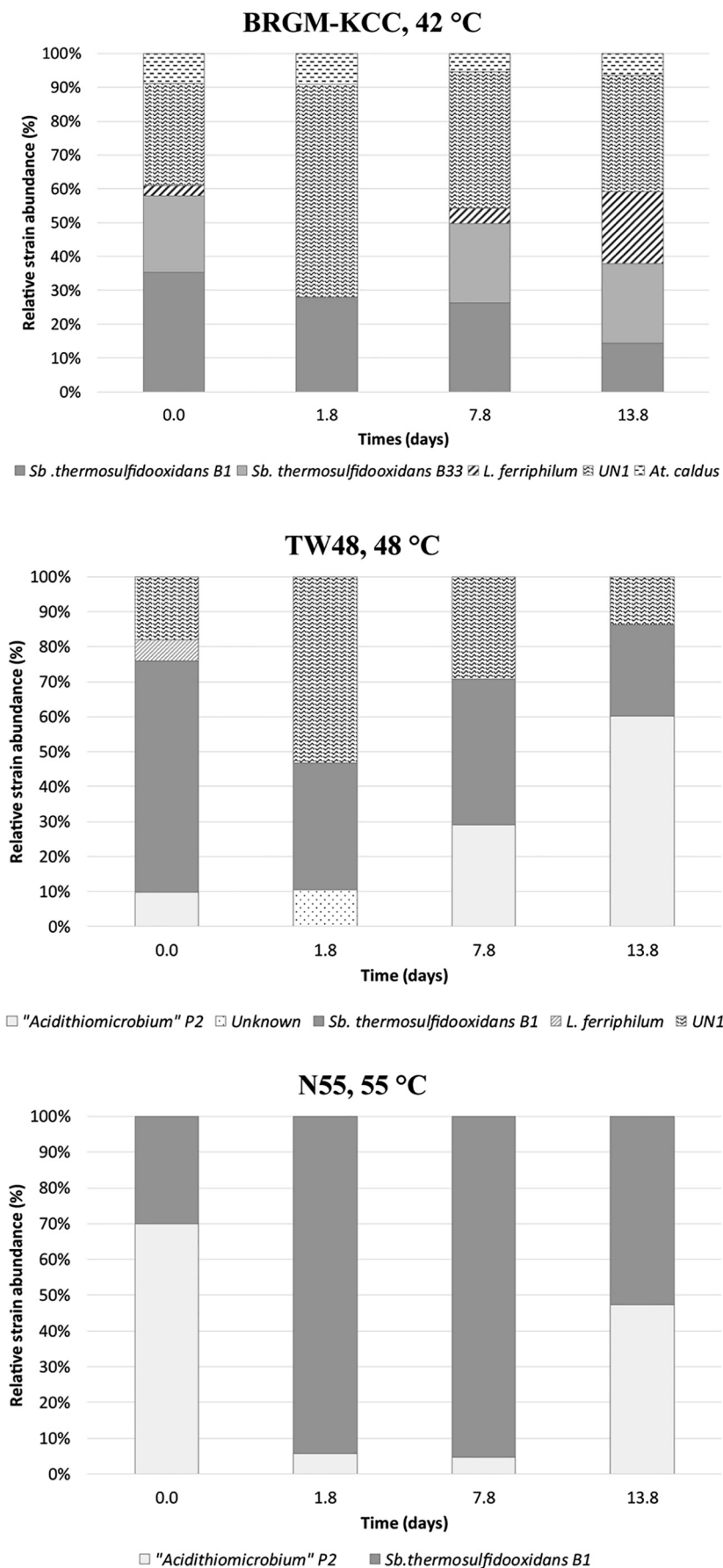


Fig. 8. Diversity fingerprints of the bacterial community in 2 L-reactors for BRGM-KCC at 42 °C, TW48 at 48 °C and N55 at 55 °C during the third subculture.

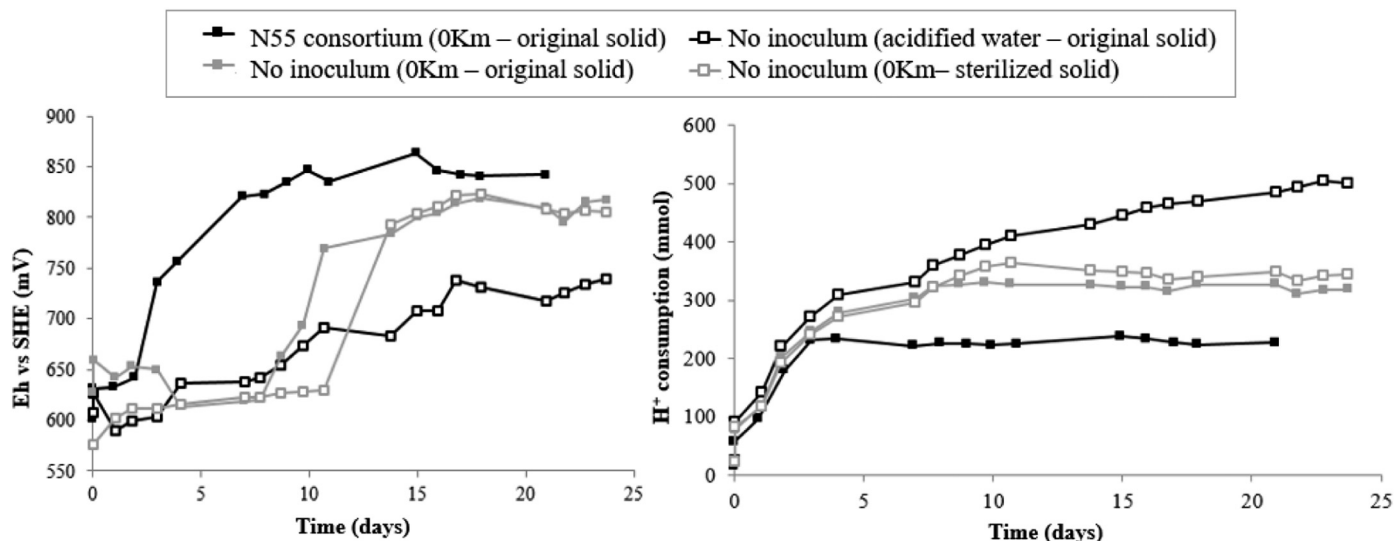


Fig. 9. Redox potential (left) and proton consumption (right) versus time in the abiotic tests with no inoculum, compared to bioleaching experiment with the N55 consortium.

The initial and fast dissolution of Ni and Zn was followed by a slower dissolution phase in which around 35% of Ni and 70% of Zn were released to solution in the biotic experiments. In this second phase, most of Ni and Zn were dissolved when the Eh was low and a small portion was dissolved after the steep increase of Eh. In the absence of added biomass (abiotic tests), Ni and Zn dissolution yields were slightly lower (25% and 60% respectively). From these results, it can be assumed that part of Ni and Zn was dissolved by acid leaching, whereas another smaller portion was likely dissolved by oxidation of Fe(III), which requires an active Fe-oxidizing biomass. In our experiments, the acid-soluble minerals include pyrrhotite and violarite (which contain Ni) and sphalerite (which contains Zn). FeS-alt detected in the mineralogical analysis of Sotkamo secondary ore would have also been a source for the Ni and Zn dissolved at low redox potential. Arpalahiti and

Lundström (2018) showed that in Sotkamo primary bioleach operation, dissolved metals could react directly with, and be taken up in, pyrrhotite due to the low redox conditions encountered in the primary heap through a phenomenon called metathesis according to the following equation (Eq. 1):



In the absence of microbial oxidizing activity, the leaching of acid soluble minerals leads to the formation of elemental sulfur which can be oxidized later when the microbial activity increases (Schippers, 2004). In the abiotic tests without nutrients, in which no active biomass developed, formation of elemental sulfur was observed, confirming this hypothesis.

The slow release of Ni at higher solution redox potentials may be

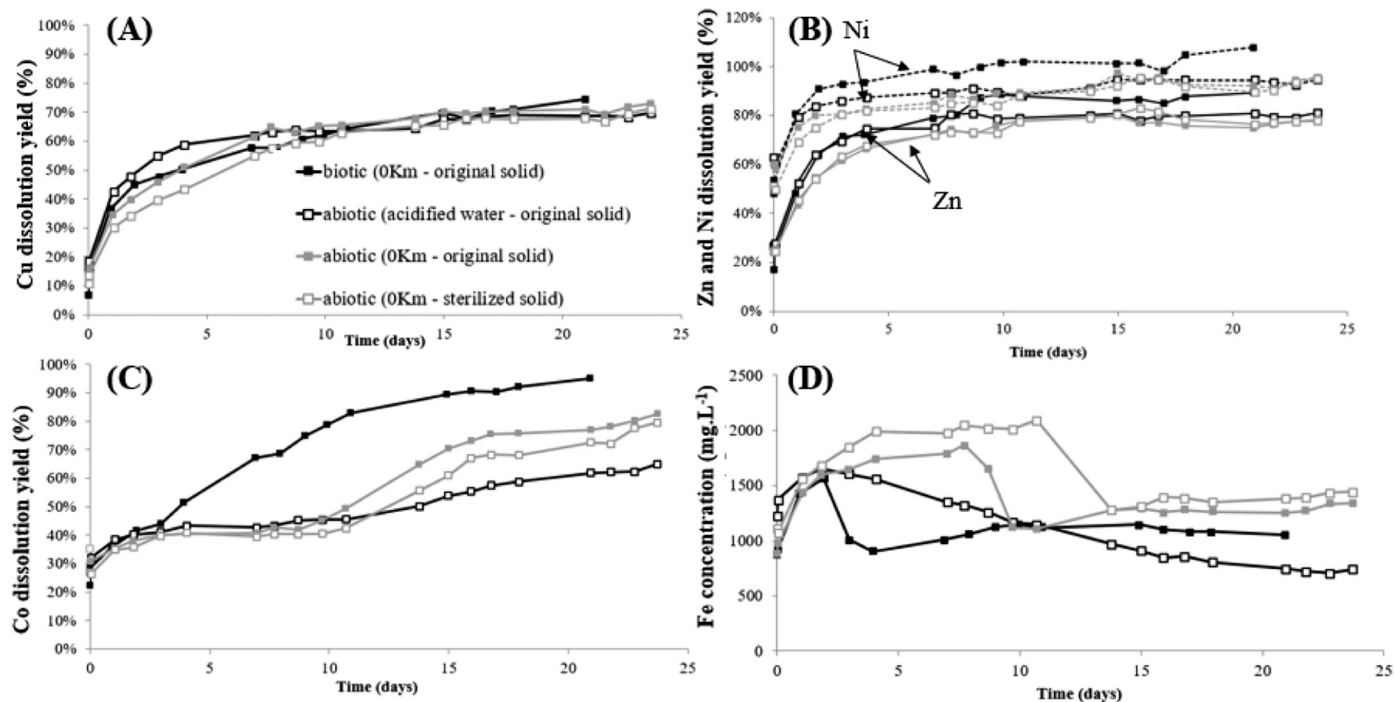


Fig. 10. (A) Cu, (B) Ni (dotted lines) and Zn (solid lines), (C) Co dissolution yields and (D) Fe concentration over time in abiotic tests, compared to the bioleaching experiment with N55 consortium.

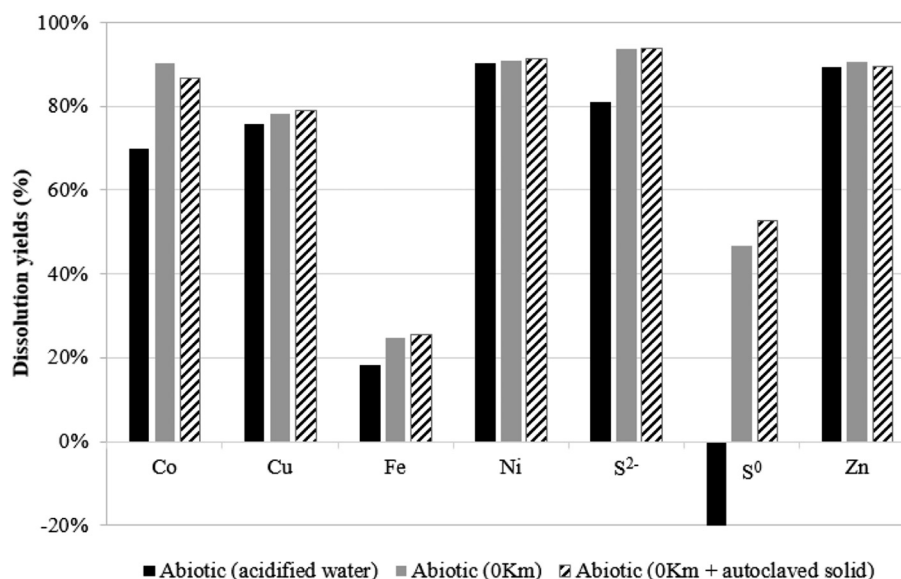


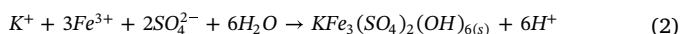
Fig. 11. Metals and sulfur dissolution yields after 24 days in abiotic experiments at 55 °C.

related to Ni release from pyrite, or to the slow dissolution of highly occluded mineral sulfides such as pentlandite and violarite.

Cobalt behaved differently to Ni and Zn. After the rapid release observed at the very beginning of the tests, Co did not enter the aqueous phase until the sharp increase of the redox potential up to 800 mV. In the abiotic tests, where the solution redox potential remained low, Co dissolution was substantially lower than in the biotic tests. This suggests that significant Co was contained in acid insoluble minerals such as pyrite, which cannot be leached rapidly without microbial Fe-oxidizing activity. The Co-bearing nature of the pyrite was confirmed by the EMPA analysis (Fig. 2).

Copper dissolution was limited (~60%), and consistent whatever the operating conditions tested in the bioleaching experiments carried out at 55 °C. The only discrete Cu-bearing mineral detected in Sotkamo secondary ore was chalcopyrite but significant copper was detected in the FeS-alt. The limited dissolution yield of chalcopyrite was probably due to its recalcitrant nature during the bioleaching tests and to its low concentration in the secondary ore (0.17 wt% which accounts for 0.06 wt% of the total Cu in the secondary ore) (Dreisinger, 2006; Kutschke et al., 2015; Watling, 2006). Our results suggest that the dissolution limitation of chalcopyrite can be partially overcome by increasing the temperature, as confirmed by the Cu leaching yields obtained at 42, 48 and 55 °C with the BRGM-KCC, TW48 and N55 consortia, respectively. However, the degree of chalcopyrite leaching is usually higher in biotic systems than in abiotic systems (Hedrich et al., 2018). This is not consistent with results obtained in this study because the Cu dissolution kinetics were almost identical in the biotic and abiotic experiments. This suggests that dissolved Cu may be attributed to the dissolution of easily leached Cu-bearing sulfates or sulfides in the secondary ore, rather than to the dissolution of residual chalcopyrite.

In parallel with these dissolution phenomena, we proposed that jarosite precipitation took place, as shown in Eq. 2.



Numerous studies have demonstrated that higher temperatures promote higher jarosite precipitation yields, as observed in our experiments (Dutrizac, 1983; Dutrizac and Jambor, 2000; Leahy and Schwarz, 2009). The precipitation of Fe was simultaneous with its dissolution from Fe-bearing sulfide minerals such as pyrrhotite and pyrite.

Although the use of different temperatures did not impact significantly the metal dissolution kinetics (apart from Cu), various

microbial communities were observed in our experiments. A lower diversity was observed at 48 and 55 °C compared to that at 42 °C. This is consistent with the composition of the initial inoculum. We suggest that increased temperatures were a significant factor reducing the diversity, especially at 55 °C, which might be too high to sustain a competitive growth of bacteria such as *L. ferriphilum* (optimal temperature at 38 °C; Coram and Rawlings, 2002) and *At. caldus* (temperature range of 32–52 °C with an optimum at 45 °C; Hallberg and Lindstrom, 1994). The dominance of *Sb. thermosulfidooxidans* and 'Acidithiomicrobium' P2 in N55 is consistent if we consider reported optimal growth of 50–55 °C for the type strain of *Sb. thermosulfidooxidans* (Golovacheva and Karavaiko, 1978) and 50 °C for 'Acidithiomicrobium' P2 (Norris et al., 2011). At 48 and 55 °C, they were the only iron-oxidizing bacteria that were detected in large proportion in the reactors, suggesting their central role in bioleaching of the Sotkamo secondary ore in moderate thermophilic conditions. These results confirmed previous conclusions carried out from continuous bioleaching experiments of Ni concentrate: Cleaver et al. (2007) detected the strain P2 together with *At. caldus* as the dominant microorganisms at 49 °C while they were replaced by *Sb. thermosulfidooxidans* at 55 °C. In this study, it is interesting to note that *At. caldus* was found at 49 °C but not at 55 °C, as was the case in our study for strain UN1, which is suspected to be an *At. caldus* strain although it could not be fully confirmed here based solely on gene fingerprints. 'Acidithiomicrobium' P2 also dominated at 47 °C in columns leaching Cu sulfide ore from the Escondida mine in Chile or polymetallic ore from the Talvivaara (now Terrafame) mine in Finland (Norris et al., 2011). In addition to these studies, our results show the capacity of 'Acidithiomicrobium' to develop also in large proportions at 55 °C.

5. Conclusion

Mine wastes are receiving renewed attention for their potential as a metal resource. Some large reprocessing operations are being developed worldwide, based on new metallurgical processes. Among them, bioleaching is emerging as an alternative for the reprocessing of sulfidic mine waste. However, two issues need to be addressed. First, the mineralogy of the wastes need to be ascertained, to accurately quantify and have knowledge on the distribution of the target elements. Secondly, optimized operating conditions need to be determined taking into account the mineralogy to obtain high dissolution kinetics, so that the process will be economically acceptable. This study aimed at

assessing the mineralogical characterization of primary heap mining residues, known as 'secondary ore' from Sotkamo (Terrafame, Finland) and at performing bioleaching experiments in STR maintained at different temperature. The goal was to combine both results to investigate the metal dissolution and precipitation mechanisms.

The use of QEMSCAN® combined with EMPA and SEM allowed the metal-bearing minerals in the secondary ore to be characterized. The mineralogy of the sample was complex, with Fe-bearing minerals (composed with FeS- alt, pyrite, pyrrhotite, violarite, Fe oxides and jarosite) and sphalerite as the main S-minerals. Metals are disseminated in numerous phases. While the highest concentrations of Ni were found in violarite, Cu in chalcopyrite, Zn in sphalerite, the FeS-alt and the FeOx were the bearers of most of the different metals (Ni, Zn, Cu, Co) although at low concentrations. The other sulfides, pyrite and pyrrhotite, contained minor amounts of Co and Cu (not in pyrite).

Bioleaching experiments were performed at three different temperatures (42, 48 and 55 °C) with three consortia and were compared to abiotic experiments at 55 °C. Substantial and rapid release of Ni, Co, Zn and Cu occurred at the very beginning of the experiments, suggesting the dissolution of soluble salts. Chemical leaching mechanisms then occurred in the bioreactors due to the presence of acid soluble sulfides (such as pyrrhotite) in the secondary ore. Large quantities of Ni and Zn were released in solution. After 3 days, once all acid soluble sulfides were leached, acid insoluble minerals such as pyrite started to dissolve due to microbial growth and activity. Cobalt and a small proportion of the Ni were leached during this period of time. Copper dissolution was slightly improved with increasing temperature and may be attributed to the dissolution of easily leached Cu-bearing phases rather than the dissolution of residual chalcopyrite. Finally, significant jarosite precipitation phenomenon was observed and increased with increasing temperature.

From the determination of these mechanisms, new opportunities are offered for better understanding of the mechanisms that are currently occurring in the secondary bioheap-leaching on site. These results may also path new ways for optimising other parameters, such as the solid concentration, for bioleaching of the secondary ore in stirred tank reactor.

Declaration of Competing Interest

The authors declare that they have no known competing financial interests or personal relationships that could have appeared to influence the work reported in this paper.

Acknowledgement

This work is part of the European collaborative research project NEMO (Near-zero-waste recycling of low-grade sulfidic mining waste for critical-metal, mineral and construction raw-material production in a circular economy), funded by the European Union's Horizon2020 research and innovation programme under grant agreement No 776846. We are grateful to M. Ville Heikkinen from Terrafame who managed the sampling and shipment of the materials from Finland to BRGM research center.

Appendix A. Supplementary data

Supplementary data to this article can be found online at <https://doi.org/10.1016/j.hydromet.2020.105484>.

References

Ahonen, L., Tuovinen, O.H., 1995. Bacterial leaching of complex sulfide ore samples in bench-scale column reactors. *Hydrometallurgy* 37, 1–21.
 Arpalahiti, A., Lundström, M., 2018. The leaching behavior of minerals from a pyrrhotite-rich pentlandite ore during heap leaching. *Miner. Eng.* 119, 116–125.

Bhatti, T.M., Bigham, J.M., Riekkola-Vanhanen, M., Tuovinen, O.H., 2010. Altered mineralogy associated with stirred tank bioreactor leaching of a black schist ore. *Hydrometallurgy* 100, 181–184.
 Bhatti, T.M., Bigham, J.M., Vuorinen, A., Tuovinen, O.H., 2012. Chemical and bacterial leaching of metals from black schist sulfide minerals in shake flasks. *Int. J. Miner. Process.* 110–111, 25–29.
 Bodéan, F., Jacob, J., Guézennec, A.G., 2018. Final Report n°BRGM/RP-67562-FR: "Revue d'expériences de retraitement de résidus miniers (Europe, Monde). Perspectives." 50 pages. (In French).
 Bransgrove, R., Rollinson, G.R., Williamson, B.J., Bryan, C.G., 2018. Analysis of Sulfidic Coal Production Wastes Using Biokinetic Tests Combined with QEMSCAN. *Sustainable Minerals '18*, Windhoek, Namibia.
 Cleaver, A.A., Burton, N.P., Norris, P.R., 2007. A novel *Acidimicrobium* species in continuous cultures of moderately thermophilic, mineral-sulfide-oxidizing acidophiles. *Appl. Environ. Microbiol.* 73 (13), 4294–4299.
 Coram, N.J., Rawlings, D.E., 2002. Molecular relationship between two groups of the genus *Leptospirillum* and the finding that *Leptospirillum ferriphilum* sp. nov. dominates South African commercial biooxidation tanks that operate at 40°C. *Appl. Environ. Microbiol.* 68 (2), 838–845.
 D'Hugues, P., Foucher, S., Gallé-Cavalloni, P., Morin, D., 2002. Continuous bioleaching of chalcopyrite using a novel extremely thermophilic mixed culture. *Int. J. Miner. Process.* 66, 107–119.
 D'Hugues, P., Joulain, C., Spolaore, P., Michel, C., Garrido, F., Morin, D.H.R., 2007. Continuous bioleaching of a cobaltiferous pyrite in stirred reactors: population dynamics and EPS production vs. bioleaching performances. *Adv. Mater. Res.* 20–21, 62–65.
 d'Hugues, P., Norris, P.R., Hallberg, K.B., Sánchez, F., Langwaldt, J., Grotowski, A., Chmielewski, T., Groudev, S., 2008. Bioshale FP6 European project: exploiting black shale ores using biotechnologies? *Miner. Eng.* 21, 111–120.
 Dew, D.W., Buuren, C.V., McEwan, K., Bowker, C., 2000. Bioleaching of base metal sulphide concentrates: a comparison of high and low temperature bioleaching. *J. South. Afr. Inst. Min. Metall.* 409–414.
 Dopson, M., Halinen, A.-K., Rahunen, N., Boström, D., Sundkvist, J.-E., Riekkola-Vanhanen, M., Kaksonen, A.H., Puhakka, J.A., 2008. Silicate mineral dissolution during heap bioleaching. *Biotechnol. Bioeng.* 99, 811–820.
 Dreisinger, D., 2006. Copper leaching from primary sulfides: options for biological and chemical extraction of copper. *Hydrometallurgy* 83, 10–20.
 Dutrizac, J.E., 1983. Factors affecting alkali jarosite precipitation. *Metall. Trans. B* 14, 531–539.
 Dutrizac, J.E., Jambor, J.L., 2000. Jarosites and their application in hydrometallurgy. In: Alpers, C.N., Jambor, J.L., Nordstrom, D.K. (Eds.), *Sulfate Minerals. Crystallography, Geochemistry and Environmental Significance*. 40. Ref. Mineral. Geochem., pp. 405–452.
 Falagán, C., Grail, B.M., Johnson, D.B., 2017. New approaches for extracting and recovering metals from mine tailings. *Miner. Eng.* 106, 71–78.
 Fonti, V., Joulain, C., Guezennec, A.G., Bryan, C.G., 2019. Bioprospecting and the microbial ecology of a coal production waste dump. In: *Proceedings of IBS 2019*. 23rd International Biohydrometallurgy Symposium, Japan.
 Gericke, M., Pinches, A., van Rooyen, J.V., 2001. Bioleaching of a chalcopyrite concentrate using an extremely thermophilic culture. *Int. J. Miner. Process.* 62, 243–255.
 Golovacheva, R.S., Karavaiko, G.I., 1978. *Sulfobacillus*, a new genus of thermophilic sporeforming bacteria. *Mikrobiologiya* 47, 815–822 (In Russian).
 Guezennec, A.-G., Bru, K., Jacob, J., d'Hugues, P., 2015. Co-processing of sulfidic mining wastes and metal-rich post-consumer wastes by biohydrometallurgy. *Miner. Eng.* 75, 45–53.
 Guezennec, A.G., Joulain, C., Jacob, J., Archane, A., Ibarra, D., de Buyer, R., Bodéan, F., D'Hugues, P., 2017. Influence of dissolved oxygen on the bioleaching efficiency under oxygen enriched atmosphere. *Miner. Eng.* 106, 64–70.
 Guezennec, A.G., Joulain, C., Delort, C., Bodéan, F., Hedrich, S., D'Hugues, P., 2018. CO₂ mass transfer in bioleaching reactors: CO₂ enrichment applied to a complex copper concentrate. *Hydrometallurgy* 180, 277–286.
 Halinen, A.-K., Rahunen, N., Kaksonen, A.H., Puhakka, J.A., 2009a. Heap bioleaching of a complex sulfide ore: part I: effect of pH on metal extraction and microbial composition in pH controlled columns. *Hydrometallurgy* 98, 92–100.
 Halinen, A.-K., Rahunen, N., Kaksonen, A.H., Puhakka, J.A., 2009b. Heap bioleaching of a complex sulfide ore: part II. Effect of temperature on base metal extraction and bacterial compositions. *Hydrometallurgy* 98, 101–107.
 Halinen, A.-K., Beecroft, N.J., Määttä, K., Nurmi, P., Laukkanen, K., Kaksonen, A.H., Riekkola-Vanhanen, M., Puhakka, J.A., 2012. Microbial community dynamics during a demonstration-scale bioheap leaching operation. *Hydrometallurgy* 125–126, 34–41.
 Hallberg, K.B., Lindstrom, E.B., 1994. Characterization of *Thiobacillus caldus* sp. nov., a moderately thermophilic acidophile. *Microbiol.* 140, 3451–3456.
 Hedrich, S., Guezennec, A.-G., Charron, M., Schippers, A., Joulain, C., 2016. Quantitative monitoring of microbial species during bioleaching of a copper concentrate. *Front. Microbiol.* 07, 2044.
 Hedrich, S., Joulain, C., Graupner, T., Schippers, A., Guézennec, A.-G., 2018. Enhanced chalcopyrite dissolution in stirred tank reactors by temperature increase during bioleaching. *Hydrometallurgy* 179, 125–131.
 Ioannou, Z., Dimirkou, A., Ioannou, A., 2013. Phosphate adsorption from aqueous solutions onto goethite, bentonite, and bentonite-goethite system. *Water Air Soil Pollut.* 224, 1374.
 Johnson, D.B., Joulain, C., d'Hugues, P., Hallberg, K.B., 2008. *Sulfobacillus benefaciens* sp. nov., an acidophilic facultative anaerobic Firmicute isolated from mineral bioleaching operations. *Extremophiles* 12, 789–798.
 Kubisz, J., 1970. Studies on synthetic alkali-hydronium jarosites. I. Synthesis of jarosite

- and natrojarosite. *Mineral. Pol.* 1, 47–57.
- Kutschke, S., Guezennec, A.G., Hedrich, S., Schippers, A., Borg, G., Kamradt, A., Gouin, J., Giebner, F., Schopf, S., Schlömann, M., Rahfeld, A., Gutzmer, J., D'Hugues, P., Pollmann, K., Dirllich, S., Bodéan, F., 2015. Bioleaching of Kupferschiefer blackshale – a review including perspectives of the Ecometals project. *Miner. Eng.* 75, 116–125.
- Lacey, D.T., Lawson, F., 1970. Kinetics of the liquid-phase oxidation of acid ferrous sulfate by the bacterium *Thiobacillus ferrooxidans*. *Biotechnol. Bioeng.* 12, 29–50.
- Leahy, M.J., Schwarz, M.P., 2009. Modelling jarosite precipitation in isothermal chalcopyrite bioleaching columns. *Hydrometallurgy* 98, 181–191.
- Lèbre, É., Corder, G., 2015. Integrating industrial ecology thinking into the management of mining waste. *Resources* 4, 765–786.
- Lottermoser, B.G., 2011. Recycling, reuse and rehabilitation of mine wastes. *Elements* 7, 405–410.
- Matinde, E., Simate, G.S., Ndlovu, S., 2018. Mining and metallurgical wastes: a review of recycling and re-use practices. *J. South. Afr. Inst. Min. Metall.* 118, 825–844.
- Miller, D.M., Dew, D.W., Norton, A.E., Johns, M.W., Cole, P.M., Benetis, G., Dry, M., 1997. The BioNIC process: description of the process and presentation of pilot plant results. In: *Proceedings for Nickel/Cobalt 1997. 36th Annual Conference of Metallurgists and the 27th Annual Hydrometallurgical Meeting of CIM, Sudbury, Canada 17–20 Aug 97.*
- Morin, D.H.R., D'Hugues, P., 2007. Bioleaching of a cobalt-containing pyrite in stirred reactors: a case study from laboratory scale to industrial application. In: Rawlings, D.E., Johnson, D.B. (Eds.), *Biomining*. Springer, Berlin, Heidelberg.
- Neale, J., Seppälä, J., Laukka, A., van Aswegen, P., Barnett, S., Gericke, M., 2017. The MONDO minerals nickel sulfide bioleach project: from test work to early plant operation. *Solid State Phenom.* 262, 28–32.
- Nemati, M., Webb, C., 1997. A kinetic model for biological oxidation of ferrous iron by *Thiobacillus ferrooxidans*. *Biotechnol. Bioeng.* 53, 478–486.
- NEMO project, 2018.** <https://h2020-nemo.eu/>.
- Niemelä, S.I., Riekkola-Vanhanen, M., Sivelä, C., Viguera, F., Tuovinen, O.H., 1994. Nutrient effect on the biological leaching of a black-schist ore. *Appl. Environ. Microbiol.* 60, 1287–1291.
- Norris, P.R., Davis-Belmar, C.S., Brown, C.F., Calvo-Bado, L.A., 2011. Autotrophic, sulfur-oxidizing actinobacteria in acidic environments. *Extremophiles* 15, 155–163.
- Norris, P.R., Laigle, L., Ogden, T.J., Gould, O.J.P., 2017. Selection of thermophiles for base metal sulfide concentrate leaching, part I: effect of temperature on copper concentrate leaching and silver recovery. *Miner. Eng.* 106, 7–12.
- Puhakka, J., Tuovinen, O.H., 1986. Microbiological solubilization of metals from complex sulfide ore material in aerated column reactors. *Acta Biotechnol.* 6, 233–238.
- Riekkola-Vanhanen, M., 2010. Talvivaara Sotkamo mine – bioleaching of a polymetallic nickel ore in subarctic climate. *Nova Biotechnol.* 10-1, 7–14.
- Rollinson, G.K., Andersen, J.C.Ø., Stickland, R.J., Boni, M., Fairhurst, R., 2011. Characterisation of non-sulphide zinc deposits using QEMSCAN®. *Miner. Eng.* 24 (8), 778–787.
- Schippers, A., 2004. Biogeochemistry of metal sulfide oxidation in mining environments, sediments, and soils. In: Amend, J.P., Edwards, K.J., Lyons, T.W. (Eds.), *Sulfur Biogeochemistry—Past and Present*. Geological Society of America, Boulder, Colorado, pp. 49–62 Special Paper 379.
- Tayebi-Khorami, M., Edraki, M., Corder, G., Golev, A., 2019. Re-thinking mining waste through an integrative approach led by circular economy aspirations. *Minerals* 9, 286.
- Watling, H.R., 2006. The bioleaching of sulphide minerals with emphasis on copper sulphides — a review. *Hydrometallurgy* 84, 81–108.
- Watling, H.R., Perrot, F.A., Shiers, D.W., 2008. Comparison of selected characteristics of *Sulfobacillus* species and review of their occurrence in acidic and bioleaching environments. *Hydrometallurgy* 93, 57–65.
- Watling, H.R., Collinson, D.M., Fjastad, S., Kaksonen, A.H., Li, J., Morris, C., Perrot, F.A., Rea, S.M., Shiers, D.W., 2014. Column bioleaching of a polymetallic ore: effects of pH and temperature on metal extraction and microbial community structure. *Miner. Eng.* 58, 90–99.